

Comparative Divertor-Transport Study for W7-AS and LHD

Y. Feng^{a)}, M. Kobayashi^{b)}, N. Ashikawa^{b)}, L. Giannone^{a)}, P. Grigull^{a)}, K. Ida^{b)}, J. Kisslinger^{a)}, A. Komori^{b)}, R. König^{a)}, LHD experimental group^{b)}, S. Masuzaki^{b)}, K. McCormick^{a)}, J. Miyazawa^{b)}, T. Morisaki^{b)}, S. Morita^{b)}, O. Motojima^{b)}, Y. Nakamura^{b)}, K. Narihara^{b)}, N. Ohyabu^{b)}, B.J. Peterson^{b)}, F. Sardei^{a)}, K. Sato^{b)}, M. Shoji^{b)}, N. Tamura^{b)}, H. Thomsen^{a)}, M. Tokitani^{b)}, F. Wagner^{a)}, U. Wenzel^{a)}, H. Yamada^{b)}, I. Yamada^{b)}

^{a)}Max-Planck-Institut für Plasmaphysik, Euratom Association, Germany

^{b)}National Institute for Fusion Science, Toki, Japan

Using the W7-AS island divertor and the helical divertor in LHD as examples, the paper presents a comparative divertor transport study, aiming at identifying the essential differences and similarities in divertor function between two typical helical devices of different size and divertor concept. Investigated are the impacts of specific field and divertor topologies on plasma, impurity and neutral transport. Topics addressed are neutral screening, impurity retention, thermal power removal via impurity line radiation, detachment and Marfes. Special attention is paid to the SOL screening effect on intrinsically-released impurities, as predicted by the EMC3/EIRENE code for both divertors. The conditions for realizing the impurity-screening regime in the SOL are analyzed and its role in achieving high-density plasmas in helical devices is assessed. Discussion is guided by EMC3/EIRENE simulations. Key physics issues are compared with experimental results.

Keywords: W7-AS, LHD, EMC3-EIRENE, Divertor, SOL transport, Impurity screening, Detachment

1. Introduction

Unlike the standard poloidal-field divertor in tokamaks, divertor concepts presently investigated in stellarators are based on specific edge magnetic field structures intrinsically available in each device [1]. Typical examples are the island divertor for the advanced low-shear stellarators W7-AS [2] and W7-X [3], and the helical divertor for the high-shear, largest heliotron-type device LHD [4]. The former utilizes the divertor potential of inherent edge magnetic islands while the latter is based on a stochastic field resulting from island overlapping. In view of the large differences in field and divertor geometry among helical devices, it is interesting to see whether there exist certain common physics issues in terms of divertor transport or divertor functionality. Recently a collaboration work between IPP and NIFS was started for this purpose and the paper presents a comparative divertor transport study for the island divertor (ID) in W7-AS and the helical divertor (HD) in LHD. Discussion throughout this paper is guided by EMC3[5]-EIRENE[6] simulations. Topics addressed are particle flux enhancement, neutral screening, impurity retention, impurity radiation and detachment, as already extensively studied for the W7-AS ID (see e.g [7]). They are also the important basic elements of a divertor which

need to be firstly investigated and understood especially for a divertor concept based on a complex 3D field structure like the ID in W7-AS and the HD in LHD. In particular, the paper is concentrated on understanding the elementary, global transport processes associated with the specific field topologies, aiming at forming a comparison basis for two typical helical devices of completely different divertor concept and geometry.

2. Divertor and field topology

W7-AS is a low-shear stellarator having a five-fold field symmetry. The low-shear in W7-AS favors large island formation as the radial size of the islands scales as $r_i \propto \sqrt{Rb_{mn}/n\iota'}$ where R is major radius, b_{mn} the resonant radial perturbation field normalized to the toroidal field, n the poloidal mode number and ι' the shear. Within the operational ι -range (0.3~0.7), a number of low-order islands of different poloidal mode numbers are available at the edge. The extensively-explored, so-called standard divertor configuration is based on the 5/9 island chain, which is shown in Figure 1. Two up/down symmetric divertor modules are installed at the elliptical plane of each field period, with five identical divertor module pairs covering the whole torus. The divertor plates are discontinuous due to technical reasons. Each

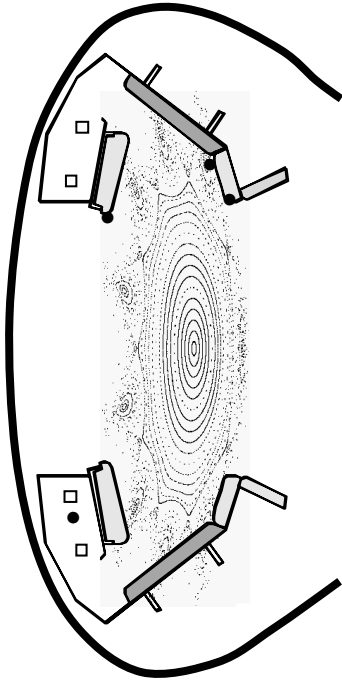


Fig.1 Standard W7-AS island divertor configuration: Nine islands are formed at the edge of the 5/9 configuration. A divertor module pair is up/down-symmetrically installed on the elliptical cross-section.

target plate toroidally extends over 18 degrees and poloidally cuts two islands in order to increase the deposition area. The baffles prevent the recycling neutrals from escaping from the divertor region towards the midplane where the magnetic islands are radially strongly compressed and optically thin for the recycling neutrals. The island size and the internal field-line pitch can be adjusted externally by ten control coils.

LHD is the largest heliotron-type device with 10 field periods. In contrast to W7-AS, LHD has a large shear, especially at the edge. The rotational transform in the edge region of the helical divertor configuration covers countless resonances which overlap each other, forming a stochastic layer of ~ 10 cm thickness. Unlike the single island chain in W7-AS, the stochastic SOL in LHD exhibits a complex field structure characterized by coexistence of remnant magnetic islands, stochastic fields and edge surface layers. Deep in the SOL, the moderate shear does not destroy the low-order islands completely, so that closed island surfaces still exist in limited regions around the O-points. Moving outwards, the shear increases quickly, leading to stronger island overlap. The remnant island cores become smaller and eventually disappear. In this case, the Chirikov parameter [8] should largely exceed unity and the field lines are then expected

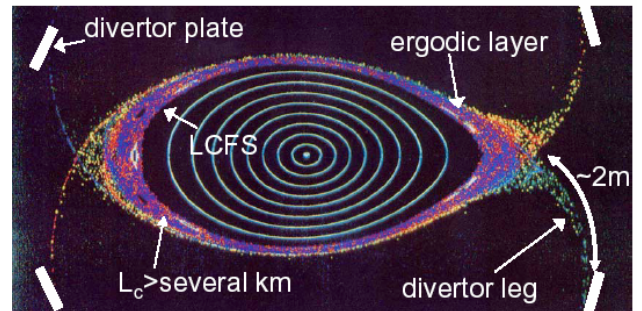


Fig. 2 Field and divertor geometry of the helical divertor in LHD.

to behave diffusively [9]. In reality, however, thin open surfaces have been identified to exist within the outer, strong island-overlapping region in LHD [4]. In the outermost region close to the wall, the increased poloidal field components of the two helical coils form a configuration similar to the double-null configuration in tokamaks, as shown in figure 2. Graphite targets cut the four divertor legs at the position just before their termination on the wall. The large poloidal component of the field along the divertor legs result in short connection lengths (~ 2 m on average) from the X-points to the targets [10]. Thus, the divertor legs are optically thin for the recycling neutrals, especially for the presently-open divertor structure.

2. Basic common transport features

Plasma transport in the island SOL of W7-AS can well be explained in terms of regular magnetic islands [7]. In order to clarify to what extent the plasma transport follows the complex field structure in LHD, EMC3/EIRENE simulations have been performed [10, 11]. In the following, we make a transport analysis based on figure 3, starting with the field topology shown in the lower picture. The 10/8 island chain has a quasi-closed island structure, which is clearly shown by the Poincare-plots. Starting from the 10/7 island chain, the field lines in the most region become irregular, with small island cores, however, remaining in the 10/7 and 10/6 island chains. Moving outwards, closed island cores vanish and Poincare-plots show a strong irregularity of the field lines, thus indicating that the field is highly stochastic. On the other hand, the underlying connection length contour plots show a strong field-line correlation even in the outer region without remnant island cores. The connection length contour reflects actually the basic field structure of low-order resonances. Indeed, all the low-order modes expected within the give r -range can be identified. This strong field-line correlation contradicts obviously the diffusive behavior of field lines characterized by

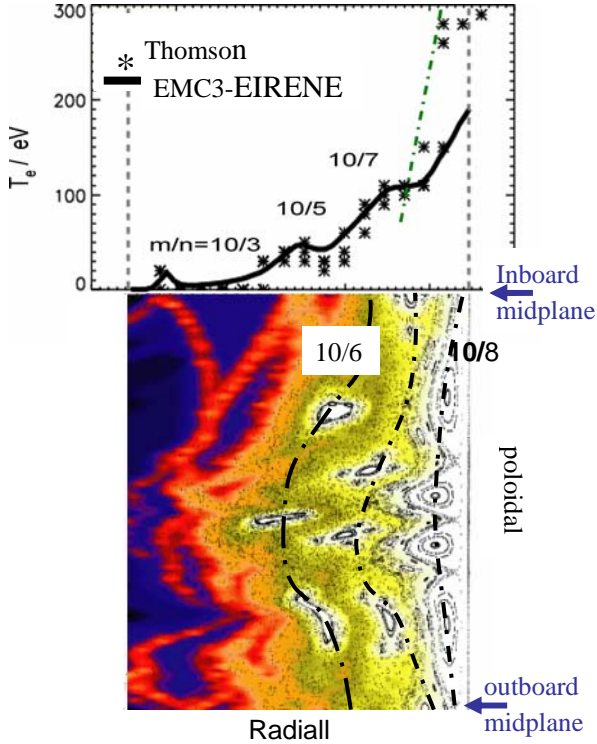


Fig.3 Comparison of T_e -profiles between simulations and Thomson measurements (upper) and a radially-zoomed connection length contour with an overlying Poincare plot (lower) over half poloidal field period at a toroidal location as shown in figure 2. The three dot-dashed lines indicate the $10/6$, $10/7$ and $10/8$ island chains which have remnant closed island cores.

ergodicity. The upper picture of figure 3 shows the calculated and measured (Thomson) T_e -profiles along the inboard midplane at a ϕ -position where the long axis of the elliptical plasma cross-section lies horizontally, as shown in figure 2. Both the code and Thomson results show clearly the impact of the low-order $10/7$, $10/5$ and $10/3$ magnetic islands on electron energy transport. The $10/8$, $10/6$ and $10/4$ mode structures have a poloidally-shifted phase distribution, with the X-points being on the midplane. This is reason why they are not reflected by the T_e -profiles. In addition, the code shows a strong correlation of parallel plasma flows with the island structure where positive and negative flows surround the O-points [11]. Even for the mode structures without a closed island core, flow channels residing on the island chains are still identifiable. Thus, it is to conclude that the plasma transport in the stochastic layer is governed by the low-order islands, although the relative importance of the stochastic effects can not yet be quantified.

Particle transport along field lines is governed by a

classical convective process, with the parallel flow velocity being determined by momentum balance. Momentum transport in both W7-AS and LHD divertor configurations is characterized by friction between opposite flows in different parts of the magnetic islands which gives rise to significant momentum loss and thereby breaks up the pressure conservation along open field lines already under low-density, high-temperature conditions without intensive plasma-neutral interaction. This can be understood qualitatively by the following pressure balance equation:

$$p(1 + M^2) = 2p_{up} - mD \int \frac{nV_{\parallel}}{\Delta_{\perp}^2} dl \quad (1)$$

where p is the total thermal pressure of ions and electrons, M the Mach number and the subscript 'up' indicates upstream. The last term on the right side of eq. (1) represents the frictional momentum loss between opposite flows separated by a characteristic perpendicular distance of Δ_{\perp} . D is the diffusivity. The integration is performed along field lines from upstream down to targets. This term is relevant for W7-AS and LHD because of the small Δ_{\perp} and the long integration (connection) length. In W7-AS, interaction between opposite flows happens in both poloidal and radial directions [7], while in LHD radial approach of counter-flows residing on neighboring island chains is the main reason for flow damping [10,11].

As a consequence, a high recycling regime as observed in tokamaks does not take place in the island/stochastic SOLs of W7-AS and LHD. Target Langmuir probes show, in consistence with H_{α} -signals, typically a roughly-linear dependence of ion saturation currents on the upstream (defined at the LCFS in the presented analysis) density up to a rollover point, as

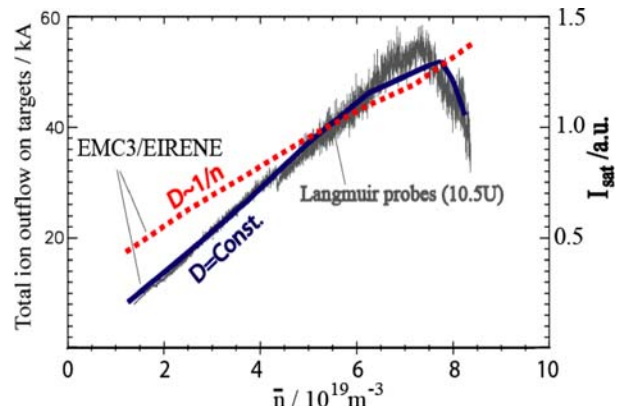


Fig. 4 Ion saturation currents increase linearly with plasma density. This linear-dependence can well be reproduced by the 3D code, independent on the D-ansatz.

shown in figure 4 for LHD. This linear behavior can be well reproduced by the EMC3/EIRENE code, insensitive to the selected D-ansatz. Nevertheless, the use of a constant D results in an ion flow slope matching better that of I_{sat} from the probes. Similar results are found in W7-AS, as shown in figure 5 where the calculated average downstream density n_{ed} is compared with those

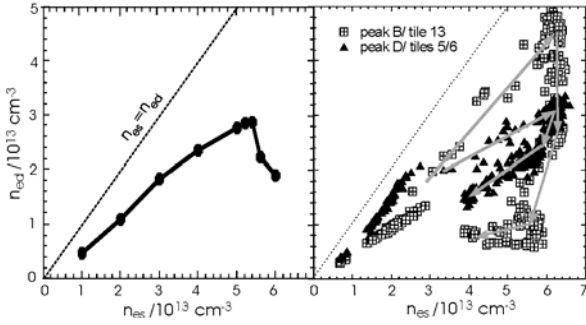


Fig.5 Absence of a high recycling regime in W7-AS, predicted by the EMC3 code (left) and confirmed by experiments (right).

from target probes of different peak locations. There is no evidence for a high recycling regime characterized by a strongly-nonlinear increase of n_{ed} with the upstream density n_{es} .

2. SOL screening effects on CX-neutrals and intrinsic impurities

Both the ID in W7-AS and the HD in LHD have an open divertor structure and the first wall is made of stainless steel. High-energetic CX-neutrals hitting the wall is a potential source producing impurities by means of physical sputtering. An optically-thick

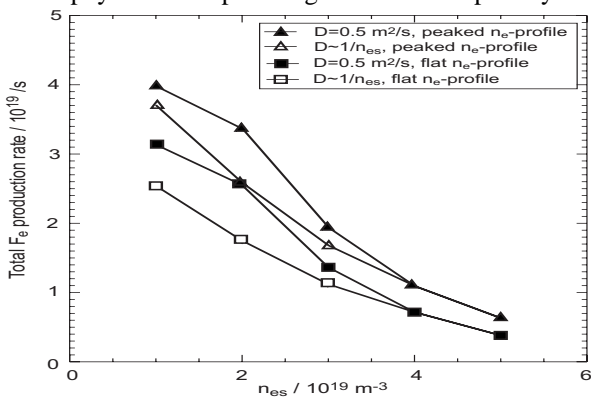


Fig.6 Sensitivities of high-energetic CX-neutrals to core profiles and cross-field transport coefficients as well as separatrix density, calculated by ECM3-EIRENE for W7-AS.

island/stochastic SOL can move the CX-neutrals to a lower energy band in the energy spectrum and thereby

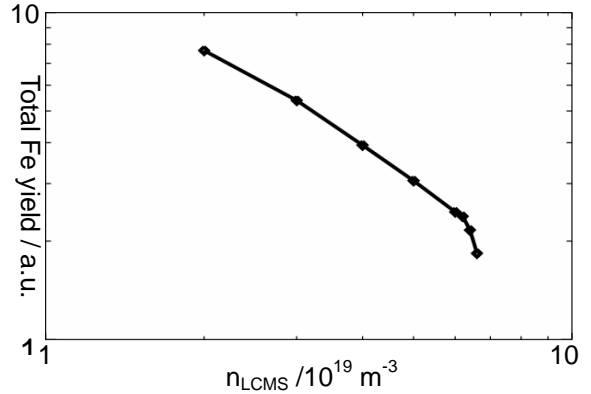


Fig.7 Calculated Fe-production rate as a function of n_{LCMS} in LHD.

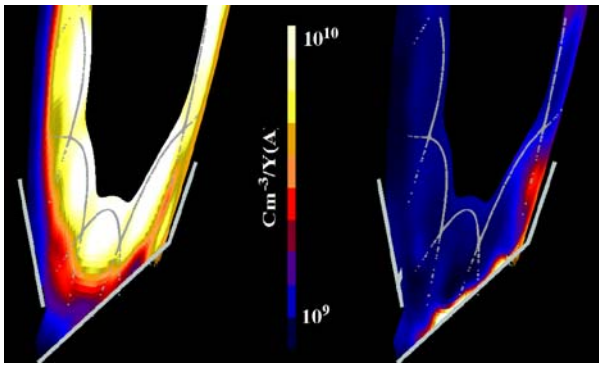
reduce the sputtering-relevant neutral flux. For a given input power entering the SOL, the SOL temperature drops with increasing the SOL density, especially at the downstream of maximum population of the recycling neutrals. Figures 6 and 7 show respectively the total Fe yield sputtered by CX-neutrals for W7-AS and LHD. Because of the existing uncertainties in wall conditioning, the Fe yield shown here should be regarded as a physics quantity for measuring the sputtering-relevant, high-energetic CX-neutral flux, rather than an absolute iron production. For both W7-AS and LHD, the 3D code simulation results show that a dense, cold island/stochastic SOL can effectively reduce the high-energetic CX-neutral flux and thereby the related Fe sputtering yield.

3. SOL impurity transport and retention

Although, as shown in the previous section, a high-density SOL moderates the physical sputtering process of CX-neutrals on plasma-facing components, high-Z impurities like the wall-released Fe can, even with a reduced source, cause significant radiation loss if they reach the confinement core region, preventing plasma from a high density operation. EMC3/EIRENE code has predicted that, under enhanced recycling conditions, the edge islands in W7-AS have a retention effect on intrinsic impurities [12]. Similar retention effect has been also predicted for the stochastic layer in LHD. Using the intrinsic carbon as test impurities, figures 8 and 9 show how the carbon impurity density distribution changes from peaked to hollow profiles with increasing the SOL density. Parallel-force balance analysis based on the 3D simulations shows that the net force acting on impurities can be, with increasing the SOL density, changed from thermal-force dominating to friction dominating, leading to a reversal of the convective impurity flow from

inwards- to outwards-directed [7, 12]. This is the reason for the carbon density profile change with the SOL density, as shown in figures 8 and 9 for W7-AS and LHD.

The reduction of the dominating ion thermal force under high SOL-density conditions are attributed to the significant contribution of the cross-field heat conduction to the energy transport in the island SOLs because of the small divertor-relevant field-line pitch in both W7-AS



a) $n_{es} = 1.5 \times 10^{19} \text{ m}^{-3}$ b) $n_{es} = 5.0 \times 10^{19} \text{ m}^{-3}$
 Fig. 8 Island retention effect on intrinsic impurities predicted for W7-AS.

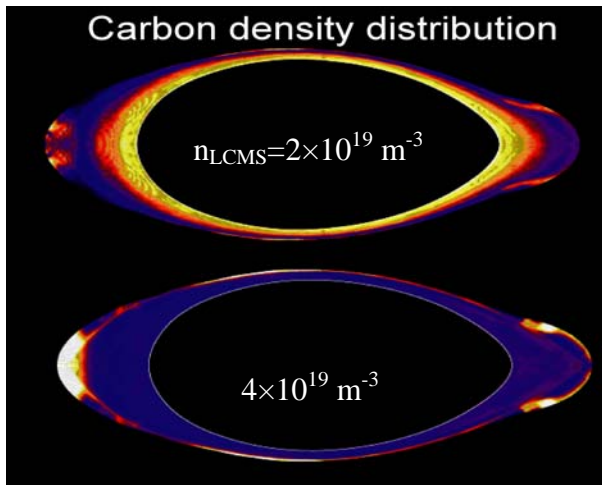


Fig. 9 Similar impurity retention effect predicted also for the stochastic layer of LHD.

and LHD. Because of the high sensitivity of the parallel heat conductivity to the ion temperature, it can be shown that, for a given input power, there exists a threshold SOL density above which the ion thermal force can be switched off and friction becomes dominating [7]. This is consistent with the experimental observations in both devices where Fe-radiation originating from core drops sharply once the plasma density is raised above a threshold density. It should be mentioned that here, a possible, still-unknown core transport mechanism setting in at high collisionalities to flush impurities could not yet be completely excluded.

A separation between core and SOL transports of intrinsic impurities has been recently realized experimentally in LHD by observing the relative changes in radiation intensity among different ionization stages of the intrinsic carbon impurities [13]. Carbon impurities of different ionization stages are populated in different depths of SOL and the radiation ratio between low and high ionization stages reflects the profile form of carbon density. Observed was a sharp decrease in the radiation ratio of high- to low-ionization stages at a SOL density roughly consistent with the code-predicted one, thus confirming the code prediction of SOL impurity retention.

4. Stability of detached plasmas

Detachment has been achieved in both devices at very high SOL densities. However, stabilizing a detached plasma turned out to be difficult. In W7-AS, stable detachment is always partial and restricted to large island and field-line pitch configurations. Configurations with small islands or field line pitch will drive detached plasmas immediately into an unstable stable, with an unstable, Marfe-like radiation inside the LCFS. In LHD, a stable partial detachment remains still a challenge and a quasi-stable complete detachment leads always to a strong degradation of the global energy confinement due to the location of a rotating radiation belt inside the LCFS. These experimental observations motivated detailed numerical studies in order to understand the underlying mechanisms driving instability. It is found numerically that the radiation distribution is highly sensitive to the

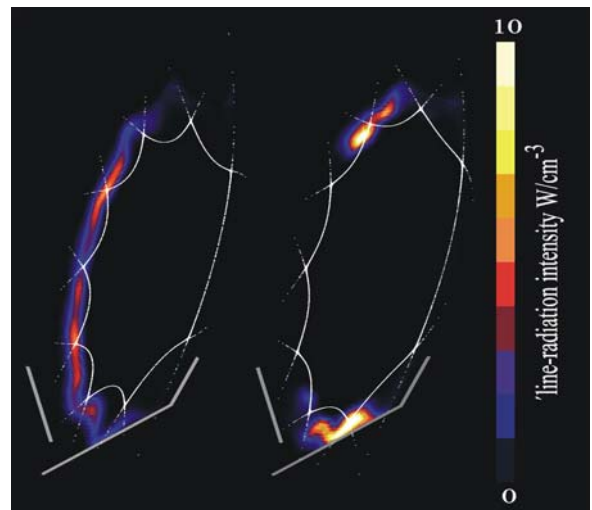


Fig. 10 Inboard side radiation (left) or divertor radiation (right), depending on the island geometry.

island geometry. For the island configurations in which stable detachment is established in W7-AS experiments,

the 3D code shows a radiation belt formed on the inboard

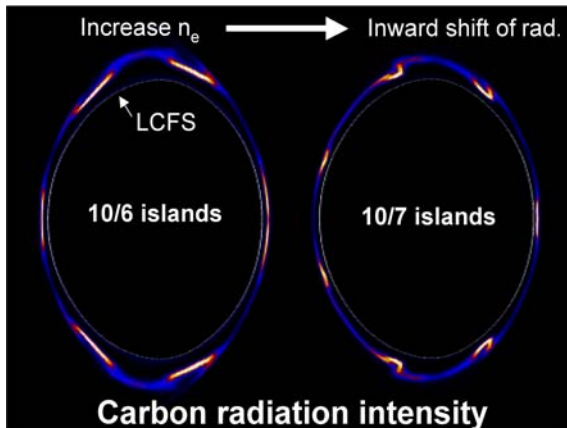


Fig. 11 Radiation prefers remnant island cores.

side (see figure 10). For small islands or field line pitch, radiation is located at the X-point in the recycling region, as shown in figure 10, leading to a strong reduction of the island neutral screening efficiency in comparison to the inboard side radiation case. A linear stability analysis shows that the loss of neutral screening could be the reason for the detachment instability observed in experiments [14]. For the stochastic layer in LHD, the 3D code predicts that remnant island cores attract radiation. Converged numerical solution is found when the radiation layer touches the 10/6 and 10/7 island chains which have small closed island cores, as shown in figure 11. Till to now, such radiation patterns could not yet be stabilized in LHD experiments. One of the possible reasons for the discrepancy, as for the divertor radiation pattern in W7-AS, is that the SOL power, which is fixed in simulations, should decrease in experiments due to the increased code density resulting from recycling neutrals after the detachment transition. The stability analysis made for W7-AS [14] should also be valid for the LHD case. More detailed analysis is left for further.

5. Conclusions

Low-order magnetic islands are the basic elements forming helical SOLs of the divertor configurations in both W7-AS and LHD. Although the large shear in LHD leads to overlapping of multi-island chains, the basic island structures of the low-order modes are not destroyed completely to allow really a diffusive approximation of field-line trajectories. EMC3-EIRENE simulations show that the SOL transport in both devices is governed by the low-order islands, which is supported by Thomson T_e -measurements in LHD. Counter plasma flows reside in different parts of the islands chains. Viscous transport due to spatial approach of the counter

flows cause significant momentum loss of the streaming ions, being the reason for the absence of a high recycling regime in both devices. It is numerically shown that a dense, cold island SOL shifts the CX-neutrals to low energy range and reduces the physical sputtering yield on plasma facing components. Benefiting from geometric advantage of the small effective field-line pitch in the islands, the parallel ion heat conductive flux can be, under high density, low temperature conditions, strongly reduced by the perpendicular one, resulting in a strong reduction of the related thermal force. Conditions for achieving a purely friction-dominated impurity transport regime are predicted by the 3D code for both W7-AS and LHD. Consistent with the code predictions, both W7-AS and LHD experiments show a sharp drop in Fe radiation from core when plasma density exceeds a threshold value. The correlation and relevance of the observations to the predicted impurity retention effect of the SOL will be checked further by isolating the SOL transport from core effects. The strong reduction of high-Z impurity concentration in the core extends the plasma to rather high densities until detachment sets in due to intensive carbon radiation. Stable partial detachment can be established in W7-AS through careful choice of the island configuration, while in LHD it is not yet successful to stabilize the radiation layer outside the confinement region. 3D simulations suggest that loss of the SOL neutral screening efficiency after detachment transition prevents the radiation layer from being stopped in the SOL. More detailed analysis on this issue is under way.

References

- [1] R. König *et al.*, *PPCF* **44**, 2365 (2002)
- [2] P. Grigull *et al.*, *PPCF* **43**, A175 (2001)
- [3] H. Renner *et al.*, *Nucl. Fusion* **40**, 1083 (2000)
- [4] N. Ohya *et al.*, *Nucl. Fusion* **34**, 387 (1994)
- [5] Y. Feng *et al.*, *J. Nucl. Mat.* **266-269**, 812 (1999)
- [6] D. Reiter, *Fusion Sci. Technol.* **47**, 172-86 (2005)
- [7] Y. Feng *et al.*, *Nucl. Fusion* **46**, 807 (2006)
- [8] B. V. Chirikov B. V., *Phys. Rep.* **52**, 265 (1960)
- [9] M. N. Rosenbluth *et al.*, *Nucl. Fusion* **6**, 297 (1996)
- [10] M. Kobayashi *et al.*, *J. Nucl. Mater.* **363-365**, 294 (2007)
- [11] Y. Feng *et al.*, "Fluid features of the stochastic layer transport in LHD", to be published in *Nucl. Fusion*, (2007)
- [12] Y. Feng *et al.*, *32nd EPS*, vol **29C** (ECA), P1.012 (2005)
- [13] M. Kobayashi *et al.*, *this conference*
- [14] Y. Feng *et al.*, *Nucl. Fusion* **45**, 89 (2005)